Physics of Plasmas

Zonal flow generation by small-scale drift-ion-acoustic waves in electron–positron–ion plasmas

Cite as: Phys. Plasmas **29**, 112109 (2022); https://doi.org/10.1063/5.0123824
Submitted: 01 September 2022 • Accepted: 12 October 2022 • Published Online: 08 November 2022

I. Javaid, L. Z. Kahlon, H. A. Shah, et al.

Physics of Plasmas ARTICLE scitation.org/journal/php

Zonal flow generation by small-scale drift-ion-acoustic waves in electron–positron–ion plasmas

Cite as: Phys. Plasmas **29**, 112109 (2022); doi: 10.1063/5.0123824
Submitted: 1 September 2022 · Accepted: 12 October 2022 ·
Published Online: 8 November 2022

I. Javaid,[1] L. Z. Kahlon,[1,a)] H. A. Shah,[1] and T. D. Kaladze[2,3]

AFFILIATIONS

[1]Physics Department, Forman Christian College (A Chartered University), Ferozpur Road, Lahore 54600, Pakistan
[2]I. Vekua Institute of Applied Mathematics, Tbilisi State University, 2 University str, Tbilisi 0186, Georgia
[3]E. Andronikashvili Institute of Physics, I. Javakhishvili Tbilisi State University, Tbilisi 0128, Georgia

[a)]**Author to whom correspondence should be addressed:** lailakahlon192@gmail.com

ABSTRACT

The generation of zonal flows by small-scale coupled drift-ion-acoustic waves is investigated. The problem is analyzed in magnetized electron–positron–ion plasmas by the system of the generalized Hasegawa–Mima equation and the equation of parallel motion of ions. It is concluded that the inclusion of positrons enhances zonal flow growth rates.

I. INTRODUCTION

The study of low-frequency coupled electrostatic drift and ion-acoustic waves (DIAWs) is of great interest because of its applications in many laboratory, space, and astrophysical systems. This problem received much attention due to the possibility of the formation of spatially three-dimensional different nonlinear solitary structures (vortices and zonal flows) in multicomponent plasmas.[1–8] The problem of coherent structures has been extensively investigated in connection with drift wave modes in tokamak plasmas. Solitary vortical structures incorporate the so-called trapped particles, and traveling vortices produce additional anomalous transport of plasma transverse to a magnetic field. The other problem that is closely connected with drift wave turbulence is the generation of sheared zonal flow spontaneously arising in laboratory plasmas as a consequence of the secondary instability of plasma due to the nonlinear interaction between the primary oscillations. Note that the existence of spatially isolated sheared zonal flows is an integral property of many planetary atmospheres and laboratory plasmas[9] controlling anomalous transport of heat and particles across the magnetic surfaces of plasma confinement systems due to the energy transport toward large-scale structures as a result of inverse energy cascade.

Nonlinear dynamics of drift waves in plasmas is primarily described by the classical Hasegawa–Mima (HM) equation[10,11] providing different structural solutions. It should be noted that the nonlinear term in the standard (classical) HM equation is expressed by the Jacobian $J(a,b) = [\nabla a \times \nabla b]_z$, where a and b are certain functions of wave field. Such nonlinearity is known as a vector nonlinearity and provides for the existence of dipolar nonlinear structures. The importance of Korteweg–de Vries (KdV) type nonlinearity $\propto \varphi^2$ in the nonlinear theory of drift waves was indicated by Petviashvili.[12] Scalar nonlinearities are responsible for the existence of monopolar nonlinear structures. The comprehensive analysis of both (monopolar and dipolar) types of drift vortical structures was given by Mikhailovskii.[13] Later, Nezlin[14] and Nezlin and Chernikov[15] elucidated the new localizing role of vector and scalar nonlinearities in the process of formation of solitary nonlinear structures and emphasized that depending on the wavelengths scale, drift waves turbulence should be described by the more complex, so-called generalized HM (GHM) equation involving both vector and scalar nonlinearity. It was elucidated that small-scale structures (compared to ion Larmor radius at the plasma electron temperature) may be described in the framework of classical HM equation containing only vector (Jacobian) nonlinearity. In other words, classical HM equation only describes small-scale dipole vortical structures. As for the large-scale electrostatic drift nonlinear waves (having dimensions larger than the characteristic Larmor radius of plasma ions) such structures may be described by a scalar nonlinearity of the KdV type. Consequently, solitary structures of the intermediate size are formed by mutual compensation of wave dispersion by both scalar and vector nonlinearities. As a result, in the general case, a solitary structure becomes essentially anisotropic and is a superposition of monopolar and dipolar vortices.

Shukla *et al.*[1] investigated linear and nonlinear properties of obliquely propagating coupled low-frequency electrostatic DIAWs in a strongly magnetized nonuniform electron–positron–ion (EPI) plasma in the presence of sheared ion flow and showed that the DIAWs can be unstable due to the ion sheared flow. Later it was shown that the nonlinear Hasegawa–Mima (HM) equation with a vector nonlinearity governing the dynamics of weakly interacting DIAWs admits vortex solutions of two different classes, viz., a vortex chain and a double vortex. Mirza and Azeem[2] presented the system of nonlinear equations, which governs the dynamics of DIAWs in a nonuniform EPI magnetoplasma with sheared ion flows. In the linear limit, a dispersion relation is obtained, which admits new instabilities of drift-waves. It is found that DIAWs can become unstable due to ion sheared flow. It is also shown that the nonlinear interactions between these finite amplitude short-wavelength waves give rise to quadrupolar vortices. Mushtaq[3] studied DIAWs stationary solitary solutions in the intermediate parametric range in both linear and nonlinear regimes in EPI magnetoplasma analytically and graphically, and it was shown that it is possible spatially limited region to derive a Zakharov–Kuznetsov equation in the nonlinear regime. Mushtaq *et al.*[4] studied linear and nonlinear DIAWs in inhomogeneous, collisional pair ion–electron plasma, and the Korteweg–de Vries–Burgers (KdVB) equation was derived and its exact solution was derived by using modified tanh–coth method for arbitrary velocity of nonlinear drift wave. Effects of species density, magnetic field, obliqueness, and the acoustic to drift velocity ratio on the solitary and shock solutions were investigated. Wang *et al.*[5] examined zonal flow (ZF) momentum balance in three-dimensional systems and DIAWs were investigated, and it was established that in a 3D system, conservation of potential vorticity (PV) is violated due to fluctuating parallel flow compressibility. The coupling between PV fluctuation and fluctuating parallel flow compression defines a source/sink for fluctuating potential enstrophy density and, thus, influences the wave momentum density modifies the zonal momentum theorem.[5] In addition, perpendicular ZFs can be excited by stationary turbulence via compressional coupling, even in the absence of a driving force and potential enstrophy flux. The coupling drive involves both perpendicular and parallel dynamics and does not require symmetry breaking in the turbulence spectrum. A new mechanism for ZF generation was, thus, revealed. Adnan *et al.*[6] investigated linear and nonlinear coupled DIAWs in a nonuniform magnetoplasma having kappa distributed electrons and positrons. In the linear regime, the role of kappa distribution and positron content on the dispersion relation was highlighted; it is found that strong superthermality and addition of positrons lowers the phase velocity due to decreasing fundamental scale lengths of the plasmas. In the nonlinear regime, first, coherent nonlinear structure in the form of dipoles and monopoles were obtained and the boundary conditions in the context of superthermality and positron concentrations were discussed. Second, in the case of scalar nonlinearity, the KdV-type equation was obtained, which admit solitary wave solution. Kaladze *et al.*[7] presented generation of sheared zonal flow by low-frequency coupled electrostatic DIAWs. Primary waves of different (small, intermediate, and large) scales are considered, and the appropriate system of equations consisting of the generalized Hasegawa–Mima equation was obtained, here the parallel ion motion was also taken into account. It is shown that along with the mean poloidal flow with strong variation in minor radius, mean sheared toroidal flow can also be generated. According to laboratory plasma experiments, main attention to large-scale DIAWs is given. Peculiarities of scalar nonlinearity due to the electrons temperature non-homogeneity in the formation of the zonal flow by large-scale turbulence are widely discussed. Namely, it is observed that such type of flows needs no generation condition and can be spontaneously excited. Kaladze *et al.*[8] obtained the GHM equation to describe the nonlinear propagation of electrostatic DIAWs in EPI plasmas. In Ref. 8, the appropriate set of 3D equations consisting of GHM equation for the electrostatic potential and equation of parallel to magnetic field motion of ions were obtained to describe the formation of coherent dipole and large-scale monopole vortices. In addition, density and temperature non-homogeneities of electrons and positrons were taken into account.

In the present work, we investigate the possibility of generation of the zonal flow for low-frequency coupled electrostatic DIAWs in an electron–positron–ion plasma and its corresponding growth rate is analyzed both analytically and numerically. We will draw our attention to the small-scale ($k_\perp \rho \gtrsim 1$, where ρ is the ion Larmor radius defined at the electron temperature) solitary structures. The parametric interaction formulation is used to investigate the instabilities of zonal flows driven by a monochromatic wave packet of primary modes. In Sec. II, the methodology leading to the system of the general Hasegawa–Mima equation for electrostatic potential and the parallel to magnetic field ion equation of motion is developed. The linear regime of the short-scale drift-ion-acoustic waves for the distinct frequencies is also discussed. In Sec. III, the possibility of sheared zonal flow generation by coupled electrostatic DIAWs for small wavelengths is discussed. In Sec. IV, the numerical approach is discussed and the enhancement of growth rate by varying distinct parameters has been shown graphically. In Sec. V, the obtained results are pointed out.

II. MATHEMATICAL FORMULATION

Let us consider low-frequency electrostatic waves in the quasi-neutral EPI plasma. We consider a local perturbation (with respect to the unperturbed plasma environment) of the plasma potential $\varphi(t, x, y, z)$ and assume that the external magnetic field $\mathbf{B}_0$ is taken in the $\hat{z}$ direction. The unperturbed plasma densities of electrons and positrons $n_{eo}(x)$, $n_{po}(x)$ and corresponding temperatures $T_{eo}(x)$, $T_{po}(x)$ are inhomogeneous and assumed to decrease monotonously along the x-axis. The ions are considered "cold" and the equilibrium quasi-neutrality condition $Zn_{i0}(x) = n_{e0}(x) - n_{p0}(x)$ is fulfilled, where Z is the charge number of positive ions.

Let us assume that in this system the plasma density perturbation arises (corresponding to the plasma-potential perturbation, φ), which excites a drift wave. Assume that the plasma motion in the (x, y)-plane is sufficiently slow so that electrons and positrons (fast moving along the magnetic field) follow the Boltzmann equilibrium. Then, from the plasma quasi-neutrality condition, the ion density is defined by the relationship

$$Zn_{i0}(x) = n_{e0}(x)\exp\left(\frac{e\varphi}{T_e(x)}\right) - n_{p0}(x)\exp\left(-\frac{e\varphi}{T_p(x)}\right). \quad (1)$$

The equation of motion for the plasma-ion component under the action of the crossed electric and magnetic, $\mathbf{B}_0$, fields has the form

$$\frac{d\mathbf{v}}{dt} = -\frac{Ze}{M}\nabla\varphi + \mathbf{v}\times\boldsymbol{\omega}_{ci}, \quad (2)$$

where $\frac{d}{dt}=\frac{\partial}{\partial t}+\mathbf{v}\cdot\nabla$, and $\mathbf{v}$, n, $\boldsymbol{\omega}_{ci}=Ze\mathbf{B}_0/M$ is the ion velocity, density, cyclotron frequency of ions, Ze and M are charge and mass of ions, respectively.

We take the drift wave's coupling with ion-acoustic ones and assume z-dependence of the fields is weak. Taking the curl of Eq. (2) and by using the equation of continuity for ions, we get[8]

$$\frac{d}{dt}\left(\frac{\boldsymbol{\Omega}+\boldsymbol{\omega}_{ci}}{n}\right)=\left(\frac{\boldsymbol{\Omega}+\boldsymbol{\omega}_{ci}}{n}.\nabla\right)\mathbf{v}, \tag{3}$$

where $\boldsymbol{\Omega}=\nabla\times\mathbf{v}$ is the vorticity. Here, the new term on the right-hand side describes vortex stretching and this equation is valid for the three-dimensional perturbations.

We also take into account the polarization drift, which is a higher order term in accordance with the ordering

$$\varepsilon\sim\frac{1}{\omega_{ci}}\frac{\partial}{\partial t}\sim\frac{1}{k_z v_{Te,p}}\frac{\partial}{\partial t}\sim\frac{\Omega}{\omega_{ci}}\sim\frac{e\varphi}{T_{e,p}}\sim\frac{a}{L}\ll 1,$$

where "a" is the perpendicular size of the structure, using the drift wave approximation[8] and L is the characteristic scale of the inhomogeneity. To express Eq. (3) in terms of potential $\varphi(x, y, z, t)$, we represent the total particle velocity as $\mathbf{v}=\mathbf{v}_\perp+e_z w$. We obtain for the perpendicular ion velocity

$$\mathbf{v}_\perp=\frac{Ze}{M\omega_{ci}}\mathbf{e}_z\times\nabla_\perp\varphi-\frac{Ze}{M\omega_{ci}^2}\left(\frac{\partial}{\partial t}+\frac{Ze}{M\omega_{ci}}\mathbf{e}_z\times\nabla_\perp\varphi.\nabla_\perp\right)\nabla_\perp\varphi, \tag{4}$$

where the subscript $\perp$ represents the plane transverse to the external magnetic field. Substituting Eqs. (1) and (4) into the z-component of Eq. (3), we get the generalized Hasegawa–Mima equation for short-scale structures having vector nonlinearity for an electron–positron–ion plasma[8]

$$\left(\frac{n_{eo}}{n_{io}}+\frac{n_{p0}}{n_{io}}\frac{T_e}{T_p}\right)\frac{\partial\varphi}{\partial t}-Z^2\rho^2\frac{\partial}{\partial t}\nabla_\perp^2\varphi-Z^2\rho^2\frac{n'_{i0}}{n_{io}}\frac{\partial^2\varphi}{\partial t\partial x}-Z^2\rho^2\omega_{ci}\frac{n'_{i0}}{n_{io}}\frac{\partial\varphi}{\partial y}-\frac{Z^3e\omega_{ci}\rho^4}{T_e}J(\varphi,\nabla_\perp^2\varphi)+\frac{ZT_e}{e}\frac{\partial w}{\partial z}=0. \tag{5}$$

From the z-component of the equation of motion (2), we get an additional equation describing the parallel to magnetic field ions motion having vector and scalar nonlinearity

$$\frac{\partial w}{\partial t}+\rho^2\omega_{ci}J(\varphi, w)=-v_s^2\frac{\partial\varphi}{\partial z}. \tag{6}$$

Here $J(a, b)=\partial_x a\partial_y b-\partial_y a\partial_x b$ is the Jacobian, $\nabla_\perp^2=\frac{\partial^2}{\partial x^2}+\frac{\partial^2}{\partial y^2}$ is the two-dimensional Laplacian, and $v_s=(T_e/M)^{1/2}$ is the ion acoustic speed. Equations (5) and (6) describe the initial closed system of equations for short-scale DIAWs which is valid for $k_\perp\rho\gg 1$. In both equations, potential φ is normalized by $\frac{T_e}{e}$.

After differentiating Eq. (5) with respect to "t" and inserting the ion parallel velocity **w** from Eq. (6), then for the propagation of DIAWs of the form $\sim e^{\mp x/2L}e^{ik_x x+ik_y y-i\omega t}$, we obtained the following dispersion equation:

$$\left(\beta+Z\rho^2\left(k_\perp^2+\frac{1}{4L^2}\right)\right)\omega_k^2-v^*k_y\omega_k-k_z^2v_s^2=0. \tag{7}$$

Here,

$$\beta=1+\frac{n_{po}}{Zn_{io}}\left(1+\frac{T_e}{T_p}\right),\quad\frac{1}{L}=-\frac{n'_{e0}-n'_{p0}}{Zn_{i0}}, \tag{8}$$

where β shows the contribution of both the number densities of electrons and positrons and their respective temperatures T_e and T_p. The term $\frac{1}{L}$ denotes inverse scale length of the inhomogeneity. The roots of dispersion equation are as follows:

$$\omega_{1,2}=\frac{v^*k_y\pm\sqrt{(v^*k_y)^2+4\left(\beta+Z\rho^2\left(k_\perp^2+\frac{1}{4L^2}\right)\right)k_z^2v_s^2}}{2\left(\beta+Z\rho^2\left(k_\perp^2+\frac{1}{4L^2}\right)\right)}, \tag{9}$$

where $v^*=Z\rho^2\omega_{ci}\left(\frac{1}{L}\right)$ is the diamagnetic drift velocity calculated at the electron temperature, $k_\perp^2=k_x^2+k_y^2$, the positive and negative signs correspond to fast and slow coupled drift ion-acoustic modes, respectively.[7,16]

The limiting cases for Eq. (9) are considered as follows:

(A) In case of $k_z=0$, we have pure single drift wave

$$\omega_k=\frac{k_yv^*}{\beta+\frac{1}{4L^2}+k_\perp^2}. \tag{10}$$

(B) In case of $k_y=0$, we have only ion-acoustic waves

$$\omega_k=\pm\frac{k_zv_s}{\sqrt{\beta+\frac{1}{4L^2}+k_\perp^2}}. \tag{11}$$

(C) For the coupled drift-ion-acoustic waves

(i) When $k_z\ll k_y$, then we have the following mixed frequencies:

$$\omega_1=\frac{k_yv^*}{\beta+\frac{1}{4L^2}+k_\perp^2}\left(1+\frac{k_z^2v_s^2}{(k_yv^*)^2}\left(\beta+\frac{1}{4L^2}+k_\perp^2\right)\right),\quad\omega_2=-\frac{k_z^2v_s^2}{k_yv^*}. \tag{12}$$

(ii) When $k_y\ll k_z$, then Eq. (9) acquires a simplified form given by

$$\omega_1=\frac{k_zv_s}{\sqrt{\beta+\frac{1}{4L^2}+k_\perp^2}}\left(1+\frac{k_yv^*}{2\left(\sqrt{\beta+\frac{1}{4L^2}+k_\perp^2}\right)k_zv_s}\right),$$
$$\omega_2=\frac{k_zv_s}{\sqrt{\beta+\frac{1}{4L^2}+k_\perp^2}}\left(-1+\frac{k_yv^*}{2\left(\sqrt{\beta+\frac{1}{4L^2}+k_\perp^2}\right)k_zv_s}\right). \tag{13}$$

III. ZONAL FLOWS IN EPI PLASMAS FOR SMALL WAVELENGTHS

In this section, we present a system of dynamic nonlinear equations that can be used to study the zonal flow generation by the coupled drift-ion-acoustic waves. In these equations, the nonlinear vector nonlinearity permits us to consider a three-wave interaction parametrically,[17]

in which the coupling between the pump electrostatic drift-ion-acoustic waves and sideband modes generates large-scale modes, called zonal flows. By normalizing time with ω_{ci}^{-1}, length by ρ, and ion parallel velocity $\mathbf{w}$ by $\rho\omega_{ci}$, Eqs. (5) and (6) can be written as

$$\begin{cases} \beta\dfrac{\partial\varphi}{\partial t}-\left(\nabla^2-\dfrac{1}{4L^2}\right)\dfrac{\partial\varphi}{\partial t}-\dfrac{1}{L}\dfrac{\partial\varphi}{\partial y}-J\left(\varphi,\nabla^2\varphi\right)+\dfrac{\partial w}{\partial z}=0,\\ \dfrac{\partial w}{\partial t}+\dfrac{\partial\varphi}{\partial z}=-J(\varphi,\,w). \end{cases} \tag{14}$$

Accordingly, perturbed quantities, i.e., the potential φ and the ion's parallel velocity $\mathbf{w}$ are divided into the following three components:

$$X=\widetilde{X}+\widehat{X}+\overline{X}, \tag{15}$$

where

$$\begin{cases} \widetilde{X}=\displaystyle\sum_{\mathbf{k}}\left[\widetilde{X}_+(\mathbf{k})\exp\left(i\mathbf{k}\cdot\mathbf{r}-i\omega_{\mathbf{k}}t\right)+\widetilde{X}_-(\mathbf{k})\exp\left(-i\mathbf{k}\cdot\mathbf{r}+i\omega_{\mathbf{k}}t\right)\right],\\ \widehat{X}=\displaystyle\sum_{\mathbf{k}}\Big[\widehat{X}_+(\mathbf{k})\exp\left(i\mathbf{k}_+\cdot r-i\omega_{\mathbf{k}+}t\right)\\ \qquad+\widehat{X}_-(\mathbf{k})\exp\left(i\mathbf{k}_-.\mathbf{r}-i\omega_{\mathbf{k}_-}t\right)+c.c.\Big],\\ \overline{X}=\overline{X}_0(\mathbf{k})\exp(-i\Omega t+iq_x x)+c.c., \end{cases} \tag{16}$$

where the symbols $\widetilde{X}$, $\widehat{X}$, and $\overline{X}$ represent the pump, the secondary small-scale modes, and the large-scale 1D zonal flow mode, respectively. Here, Ω and q_x are the frequency and wave number of the zonal flow, respectively, and c.c. stands for complex conjugative. The zonal flow mode amplitude $\overline{X}_0$ is considered uniform within the local approximation.

The following conservation laws are fulfilled between three waves: $\omega_\pm=\mathbf{\Omega}\pm\omega_k$ and $\mathbf{k}_\pm=q_x\hat{e}_x\pm\mathbf{k}$. There exist small parameters

$$\frac{|\Omega|}{|\omega_k|}\sim\frac{|q_x|}{|k_\perp|}\ll 1, \tag{17}$$

which are typical condition for zonal flow generation.[17]

By substituting Eq. (16) into the dimensionless system of Eq. (14), using the condition (17) and by neglecting the contribution of small nonlinear terms from the system of pump DIAWs modes, we get the normalized dispersion relation by averaging over fast small fluctuations. The following basic system of equations describing the evolution of mean electrostatic potential and parallel to magnetic field flows is obtained:

$$\begin{cases} -i\Omega\overline{\varphi}_0=R_\perp=-\dfrac{q_x^2}{\beta+\left(q_x^2+\dfrac{1}{4L^2}\right)}\displaystyle\sum_k k_y r_\perp(\mathbf{k}),\\ -i\Omega\,\overline{w}_0=R_\parallel=q_x\textstyle\sum_k k_y r_\parallel(\mathbf{k}), \end{cases} \tag{18}$$

where

$$r_\perp(\mathbf{k})=\widehat{\chi}_+\widetilde{\varphi}_--\widehat{\chi}_-\widetilde{\varphi}_+,\quad r_\parallel(\mathbf{k})=\widehat{\lambda}_+\widetilde{\varphi}_--\widehat{\lambda}_-\widetilde{\varphi}_+. \tag{19}$$

On the right-hand sides of Eq. (18), we get the driving forces of zonal flows, which are the mean electrostatic Reynolds stress $r_\perp$ and the electromotive force $r_\parallel$, respectively. Note that the second equation in (19) is the evolutionary equation of the parallel to magnetic field mean flow. Auxiliary sideband amplitudes in Eq. (19) are determined by

$$\widehat{\chi}_\pm=q_x\widehat{\varphi}_\pm\pm 2k_x\widehat{\varphi}_\pm,\quad \widehat{\lambda}_\pm=\widehat{w}_\pm-\frac{\mathbf{k_z}}{\boldsymbol{\omega}_\mathbf{k}}\widehat{\varphi}_\pm. \tag{20}$$

To calculate these driving forces, we need to calculate sideband amplitudes. For these amplitudes, we get the following system of equations:

$$\begin{cases} \left[\omega_\pm\left(\beta+k_{\perp\pm}^2+\dfrac{1}{4L^2}\right)\mp\left(\dfrac{1}{L}\right)k_y\right]\widehat{\varphi}_\pm\mp k_z\widehat{w}_\pm\\ \qquad=\mp i\left(q_x^2-k_\perp^2\right)k_y q_x\widetilde{\varphi}_\pm\overline{\varphi}_0,\\ \omega_\pm\widehat{w}_\pm=\mp i\left(\overline{w}_0-\dfrac{k_z}{\omega_k}\overline{\varphi}_0\right)k_y q_x\widetilde{\varphi}_\pm\pm k_z\widehat{\varphi}_\pm. \end{cases} \tag{21}$$

The solution of the system (21) gives the amplitudes of the potential $\widehat{\varphi}_\pm$ and the z components of the velocity $\widehat{w}_\pm$ of the sideband modes, respectively.

$$\begin{cases} \widehat{\varphi}_\pm=i\dfrac{k_y q_x\widetilde{\varphi}_\pm}{D_\pm}\left\{-k_z\overline{w}_0+\overline{\varphi}_0\left[\dfrac{k_z^2}{\omega_k}\mp\omega_\pm\left(q_x^2-k_\perp^2\right)\right]\right\}\\ \widehat{w}_\pm=i\dfrac{k_y q_x\widetilde{\varphi}_\pm}{D_\pm}\left[\mp\overline{w}_0\left[\omega_\pm\left(\beta+k_{\perp\pm}^2+\dfrac{1}{4L^2}\right)\mp\left(\dfrac{1}{L}\right)k_y\right]\right.\\ \qquad\left.\pm\overline{\varphi}_0\dfrac{k_z}{\omega_k}\left[\omega_\pm\left(\beta+k_{\perp\pm}^2+\dfrac{1}{4L^2}\right)\mp\left(\dfrac{1}{L}\right)k_y\right.\right.\\ \qquad\left.\left.\mp\left(q_x^2-k_\perp^2\right)\omega_k\right]\right], \end{cases} \tag{22}$$

where

$$D_\pm=\omega_\pm^2\left(\beta+k_{\perp\pm}^2+\frac{1}{4L^2}\right)\mp\omega_\pm\left(\frac{1}{L}\right)k_y-k_z^2. \tag{23}$$

We rewrite Eq. (23) as

$$D_\pm=\pm D^{(1)}+D^{(2)}\pm D^{(3)}+D^{(4)}, \tag{24}$$

where the superscripts "(1), (2),…" show the order with respect to q_x and Ω, and

$$\begin{cases} D^{(1)}=2q_x k_x\omega_k^2+2\Omega\omega_k\left(\beta+\dfrac{1}{4L^2}+k_\perp^2\right)-\left(\dfrac{1}{L}\right)k_y\Omega,\\ D^{(2)}=\Omega^2\left(\beta+k_\perp^2+\dfrac{1}{4L^2}\right)+q_x^2\omega_k^2+4\Omega\omega_k q_x k_x,\\ D^{(3)}=2q_x\Omega^2k_x+2\Omega\omega_k q_x^2,\\ D^{(4)}=q_x^2\Omega^2. \end{cases} \tag{25}$$

Finally, we have the expressions for $r_\parallel$ and $r_\perp$ by substituting Eq. (20) in Eq. (19) under the condition (17)

$$r_{||}(\mathbf{k}) = \frac{i\,q_x k_y \Omega}{D^{(1)2}} I_k \left\{ \overline{\varphi}_0 \frac{k_z}{\omega_k} \left[-\Omega^2 \left(\beta + \frac{1}{4L^2} + k_\perp^2\right)\left(\beta + \frac{1}{4L^2}\right) + q_x^2\left(k_z^2 + \omega_k^2\left(k_\perp^2 - 4k_x^2\right)\right) + \frac{2\Omega q_x k_x}{\omega_k}\left(k_z^2 - 2\omega_k^2\left(\beta + \frac{1}{4L^2}\right)\right)\right] \right.$$
$$\left. + \overline{w}_0 \left[\Omega^2 \left(\beta + \frac{1}{4L^2} + k_\perp^2\right)^2 + q_x^2\left[4k_x^2\omega_k^2 - k_z^2\right] + 2\Omega q_x k_x \left(\omega_k\left(\beta + \frac{1}{4L^2} + k_\perp^2\right) + \left(\frac{1}{L}\right)k_y\right)\right]\right\}, \tag{26}$$

$$r_\perp(\mathbf{k}) = -\frac{i\,q_x k_y I_k \Omega}{D^{(1)2}} \left\{ \overline{\varphi}_0 \left[q_x \left(\omega_k^2 k_\perp^2 \left(\beta + \frac{1}{4L^2} + k_\perp^2\right) - 4k_x^2\omega_k^2 k_\perp^2 - 8k_x^2 k_z^2 + \frac{k_z^4}{\omega_k^2} + k_z^2\left(\beta + 2k_\perp^2 + \frac{1}{4L^2}\right)\right) - 2\Omega k_x \frac{k_z^2}{\omega_k}\left(\beta + \frac{1}{4L^2}\right)\right] \right.$$
$$\left. + \overline{w}_0 k_z \left[2\Omega k_x \left(\beta + \frac{1}{4L^2} + k_\perp^2\right) + q_x\left(-\frac{k_z^2}{\omega_k} - \omega_k\left(\beta + \frac{1}{4L^2} + k_\perp^2\right) + 8k_x^2\omega_k\right)\right]\right\}. \tag{27}$$

Here, $I_k = 2\widetilde{\varphi}_+\widetilde{\varphi}_- = 2\left|\widetilde{\varphi}_+\right|^2$ is the intensity of pumping modes. Using Eqs. (26) and (27) into Eq. (18) gives the following system of coupled linear equations for the mean electrostatic potential $\overline{\varphi}_0$ and parallel to external magnetic field motion $\overline{w}_0$:

$$\begin{cases} \overline{\varphi}_0 = I_\perp^\varphi \overline{\varphi}_0 + I_\perp^w \overline{w}_0 \\ \overline{w}_0 = I_{||}^\varphi \overline{\varphi}_0 + I_{||}^w \overline{w}_0 \end{cases}. \tag{28}$$

Here, $I_\perp^\varphi, I_\perp^w, I_{||}^\varphi, I_{||}^w$ can be called the transport coefficients, given as

$$I_\perp^\varphi = -\frac{q_x^3}{\beta + q_x^2 + \frac{1}{4L^2}} \sum_k \frac{k_y^2 I_k}{D^{(1)2}} \left\{ q_x \left[\omega_k^2 k_\perp^2 \left(\beta + \frac{1}{4L^2} + k_\perp^2\right) - 4k_x^2\omega_k^2 k_\perp^2 - 8k_x^2 k_z^2 + \frac{k_z^4}{\omega_k^2} + k_z^2\left(\beta + \frac{1}{4L^2} + 2k_\perp^2\right)\right] - 2\Omega k_x \frac{k_z^2}{\omega_k}\left(\beta + \frac{1}{4L^2}\right)\right\}, \tag{29}$$

$$I_\perp^w = -\frac{q_x^3}{\beta + q_x^2 + \frac{1}{4L^2}} \sum_k \frac{k_y^2 k_z I_k}{D^{(1)2}} \left\{ 2\Omega k_x \left(\beta + \frac{1}{4L^2} + k_\perp^2\right) + q_x \left[-\frac{k_z^2}{\omega_k} - \omega_k\left(\beta + \frac{1}{4L^2} + k_\perp^2\right) + 8k_x^2\omega_k\right]\right\}, \tag{30}$$

$$I_{||}^\varphi = -q_x^2 \sum_k \frac{k_y^2 k_z I_k}{\omega_k D^{(1)2}} \left\{ -\Omega^2 \left(\beta + \frac{1}{4L^2} + k_\perp^2\right)\left(\beta + \frac{1}{4L^2}\right) + q_x^2\left[k_z^2 + \omega_k^2\left(k_\perp^2 - 4k_x^2\right)\right] + \frac{2\Omega q_x k_x}{\omega_k}\left[k_z^2 - 2\omega_k^2\left(\beta + \frac{1}{4L^2}\right)\right]\right\}, \tag{31}$$

$$I_{||}^w = -q_x^2 \sum_k \frac{k_y^2 I_k}{D^{(1)2}} \left\{ \Omega^2 \left(\beta + \frac{1}{4L^2} + k_\perp^2\right)^2 + q_x^2\left[4k_x^2\omega_k^2 - k_z^2\right] + 2\Omega q_x k_x \left[\omega_k\left(\beta + \frac{1}{4L^2} + k_\perp^2\right) + \left(\frac{1}{L}\right)k_y\right]\right\}. \tag{32}$$

We express $D^{(1)}$ in terms of the group velocity

$$D^{(1)} = \left[2\omega_k\left(\beta + \frac{1}{4L^2} + k_\perp^2\right) - \left(\frac{1}{L}\right)k_y\right](\Omega - q_x V_g), \tag{33}$$

with

$$V_g = \frac{\partial \omega_k}{\partial k_x} = -\frac{2k_x\omega_k^2}{2\omega_k\left(\beta + \frac{1}{4L^2} + k_\perp^2\right) - \left(\frac{1}{L}\right)k_y}, \tag{34}$$

being the pump wave group velocity of drift-ion-acoustic waves.

For the system (28), the zonal flow dispersion equation is given as follows:

$$1 - \left(I_\perp^\varphi + I_{||}^w\right) + I_\perp^\varphi I_{||}^w - I_\perp^w I_{||}^\varphi = 0. \tag{35}$$

For the pump monochromatic wave packet, i.e., we consider a single wave vector on the right-hand sides of Eqs. (29)–(32). Thus, the right-hand sides of these expressions are relevant only in the case if the value $\Omega - q_x V_g$, is a small parameter. Then, the coefficients (29)–(32) can be calculated at $\Omega \approx q_x V_g$. We find

$$(\Omega - q_x V_g)^2 I_\perp^\varphi|_{\Omega = q_x V_g} = -\frac{q_x^4 k_y^2 I_k}{\left[\left(\frac{1}{L}\right)k_y - 2\omega_k\left(\beta + \frac{1}{4L^2} + k_\perp^2\right)\right]^3} \left\{ \left(\frac{1}{L}\right)^3 k_y^3 + \left(\frac{1}{L}\right)^2 k_y^2\omega_k \left[8k_x^2 - k_\perp^2 - 5\left(\beta + \frac{1}{4L^2} + k_\perp^2\right)\right] \right.$$
$$+ 4\left(\frac{1}{L}\right)k_y\omega_k^2 \left[k_x^2\left(\beta + \frac{1}{4L^2} - k_\perp^2\right) + 2\left(\beta + \frac{1}{4L^2} + k_\perp^2\right)^2 + \left(\beta + \frac{1}{4L^2} + k_\perp^2\right)\left(k_\perp^2 - 6k_x^2\right)\right]$$
$$\left. + 4\omega_k^3\left(\beta + \frac{1}{4L^2} + k_\perp^2\right)\left[\left(\beta + \frac{1}{4L^2} + k_\perp^2\right)\left(4k_x^2 - k_\perp^2\right) + k_x^2\left(2k_\perp^2 - \left(\beta + \frac{1}{4L^2}\right)\right) - \left(\beta + \frac{1}{4L^2} + k_\perp^2\right)^2\right]\right\}, \tag{36}$$

$$(\Omega - q_x V_g)^2 I_\perp^w|_{\Omega=q_x V_g} = -\frac{q_x^4 k_y^2 k_z I_k}{\left[\left(\frac{1}{L}\right)k_y - 2\omega_k\left(\beta + k_\perp^2 + \frac{1}{4L^2}\right)\right]^3}\left\{\left(\frac{1}{L}\right)^2 k_y^2 + 4\left(\frac{1}{L}\right)k_y\omega_k\left[2k_x^2 - \left(\beta + \frac{1}{4L^2} + k_\perp^2\right)\right] + 4\omega_k^2\left(\beta + k_\perp^2 + \frac{1}{4L^2}\right)\left[\left(\beta + \frac{1}{4L^2} + k_\perp^2\right) - 3k_x^2\right]\right\}, \quad (37)$$

$$(\Omega - q_x V_g)^2 I_\parallel^\varphi|_{\Omega=q_x V_g} = -\frac{q_x^4 k_y^2 k_z I_k}{\left[\left(\frac{1}{L}\right)k_y - 2\omega_k\left(\beta + k_\perp^2 + \frac{1}{4L^2}\right)\right]^4}\left\{-\left(\frac{1}{L}\right)^3 k_y^3 - \left(\frac{1}{L}\right)^2 k_y^2\omega_k\left[\left(\beta + \frac{1}{4L^2}\right) + 8k_x^2 - 6\left(\beta + \frac{1}{4L^2} + k_\perp^2\right)\right] + 4\left(\frac{1}{L}\right)k_y\omega_k^2\left[-2k_x^2\left(\beta + \frac{1}{4L^2}\right) - 3\left(\beta + \frac{1}{4L^2} + k_\perp^2\right)^2 + \left(\beta + \frac{1}{4L^2} + 7k_x^2\right)\left(\beta + k_\perp^2 + \frac{1}{4L^2}\right)\right] - 4\omega_k^3\left(\beta + \frac{1}{4L^2} + k_\perp^2\right)\left[\left(\beta + \frac{1}{4L^2} + k_\perp^2\right)\left(\beta + \frac{1}{4L^2} + 6k_x^2\right) - 3k_x^2\left(\beta + \frac{1}{4L^2}\right) - 2\left(\beta + \frac{1}{4L^2} + k_\perp^2\right)^2\right]\right\}, \quad (38)$$

$$(\Omega - q_x V_g)^2 I_\parallel^w|_{\Omega=q_x V_g} = -\frac{q_x^4 k_y^2 \omega_k I_k}{\left[\left(\frac{1}{L}\right)k_y - 2\omega_k\left(\beta + k_\perp^2 + \frac{1}{4L^2}\right)\right]^4}\left\{\left(\frac{1}{L}\right)^3 k_y^3 + \left(\frac{1}{L}\right)^2 k_y^2\omega_k\left[8k_x^2 - 5\left(\beta + \frac{1}{4L^2} + k_\perp^2\right)\right] + 4\left(\frac{1}{L}\right)k_y\omega_k^2\left(\beta + \frac{1}{4L^2} + k_\perp^2\right)\left[-5k_x^2 + 2\left(\beta + \frac{1}{4L^2} + k_\perp^2\right)\right] + 4\omega_k^3\left(\beta + \frac{1}{4L^2} + k_\perp^2\right)^2\left[3k_x^2 - \left(\beta + \frac{1}{4L^2} + k_\perp^2\right)\right]\right\}. \quad (39)$$

This gives, $I_\perp^\varphi I_\parallel^w - I_\perp^w I_\parallel^\varphi = 0$ in the zonal flow dispersion relation given by Eq. (35); therefore, Eq. (35) reduces to

$$1 - \left(I_\perp^\varphi + I_\parallel^w\right) = 0. \quad (40)$$

Using Eqs. (36) and (39), we get the following general expression for the squared zonal flow growth rate:

$$(\Omega - q_x V_g)^2 = -\Gamma^2, \quad (41)$$

where

$$\Gamma^2 = \frac{q_x^4 k_y^2 I_k \omega_k^4}{\left[k_z^2 + \omega_k^2\left(\beta + \frac{1}{4L^2} + k_\perp^2\right)\right]^4}\left\{\left[\left(\frac{1}{L}\right)k_y - 2\omega_k\left(\beta + \frac{1}{4L^2} + k_\perp^2\right)\right]^4 + \left(\frac{1}{L}\right)^3 k_y^3\omega_k\left[8k_x^2 + 1 + \left(\beta + \frac{1}{4L^2}\right)\right] + 4\left(\frac{1}{L}\right)k_y\omega_k k_z^2\left[\left(\beta + \frac{1}{4L^2} + k_\perp^2\right)(5 + 8k_x^2) + 12k_x^2k_\perp^2\right] + \omega_k^2\left[\left(\frac{1}{L}\right)^2 k_y^2 - 4\omega_k^2\left(\beta + \frac{1}{4L^2} + k_\perp^2\right)^2\right]\left[\left(\beta + \frac{1}{4L^2} + k_\perp^2\right)(9 + 4k_x^2) + 32k_x^2k_\perp^2 + 8k_x^2 - 8k_x^2\left(\beta + \frac{1}{4L^2}\right)\right] + 4\omega_k^4\left(\beta + \frac{1}{4L^2} + k_\perp^2\right)^2\left[\left(\beta + \frac{1}{4L^2} + k_\perp^2\right)(8 + k_x^2) + 23k_x^2k_\perp^2 + 11k_x^2 - 11k_x^2\left(\beta + \frac{1}{4L^2}\right) - 2\left(\beta + \frac{1}{4L^2}\right)\left(\beta + \frac{1}{4L^2} + k_\perp^2\right)\right]\right\}. \quad (42)$$

We note here that in the absence of positrons for EPI plasmas, $\beta \to 1, \frac{1}{4L^2} \to 0$ our results reduce to Eq. (58) of Ref. 7.

We consider three limiting cases here: first, when $k_z = 0$ (drift wave), second for slow branch of coupled drift-ion-acoustic waves, and third, when $k_y = 0$.

(1) For a single drift waves only ($k_z = 0$ and $\omega_1 = \frac{k_y v^*}{\beta + \frac{1}{4L^2} + k_\perp^2}$), we get

$$\Gamma^2 = \frac{q_x^4 k_y^2 I_k k_\perp^2}{\left(\beta + \frac{1}{4L^2} + k_\perp^2\right)^2}\left[6 - 5\left(\beta + \frac{1}{4L^2}\right) - 3k_x^2 + k_y^2 - \frac{6}{k_\perp^2}\left(\beta + \frac{1}{4L^2}\right)^2 + \frac{6}{k_\perp^2}\left(\beta + \frac{1}{4L^2}\right) + \frac{20k_x^2}{k_\perp^2} - \frac{20k_x^2}{k_\perp^2}\left(\beta + \frac{1}{4L^2}\right)\right]. \quad (43)$$

Therefore, the instability condition can be expressed as

$$6 + k_y^2 + \frac{6}{k_\perp^2}\left(\beta + \frac{1}{4L^2}\right) + \frac{20k_x^2}{k_\perp^2} > 5\left(\beta + \frac{1}{4L^2}\right) + 3k_x^2 + \frac{6}{k_\perp^2}\left(\beta + \frac{1}{4L^2}\right)^2 + \frac{20k_x^2}{k_\perp^2}\left(\beta + \frac{1}{4L^2}\right). \quad (44)$$

The instability condition is the same as the electron–ion plasma case discussed in Ref. 7 if the effect of positrons is neglected in the term $(\beta + \frac{1}{4L^2})$ and the fastest growth rate is obtained when $k_x = 0$.

(2) For the slow branches of the coupled drift-ion-acoustic waves:

(i) In case of $k_z \ll k_y$ where $(k_z \to 0)$, for ω_1, we get analogous growth rate of purely drift wave and for $\omega_2 = -\frac{k_z^2}{k_y \nu^*}$, we get maximum value of the growth rate

$$\Gamma^2 = q_x^4 k_y^2 I_k. \tag{45}$$

So, unlike (44), the instability in this case needs no excitation condition (i.e., exists spontaneously) and the growth rate does not depend on k_z.

(ii) In case of $k_y \ll k_z$, for $\omega_{1,2} = \pm \frac{k_z}{\sqrt{\beta + \frac{1}{4L^2} + k_\perp^2}}$, where $(k_y \to 0)$ we get the growth rate of the case 3.

(3) For a single ion-acoustic branch $\omega_{1,2} = \pm \frac{k_z}{\sqrt{\beta + \frac{1}{4L^2} + k_\perp^2}}$,

$$\Gamma^2 = \frac{q_x^4 k_y^2 I_k}{4\left(\beta + \frac{1}{4L^2} + k_\perp^2\right)^2}\left[\left(\beta + \frac{1}{4L^2} + k_\perp^2\right)\left(2\left(\beta + \frac{1}{4L^2}\right)\right.\right.$$
$$\left.\left. -1 + k_x^2 + 4k_y^2\right) - k_x^2\left(9k_\perp^2 - 3\left(-1 + \beta + \frac{1}{4L^2}\right)\right)\right]. \tag{46}$$

The instability condition is given by

$$\left[\left(\beta + \frac{1}{4L^2} + k_\perp^2\right)\left(2\left(\beta + \frac{1}{4L^2}\right) - 1 + k_x^2 + 4k_y^2\right)\right.$$
$$\left. > k_x^2\left(9k_\perp^2 - 3\left(-1 + \beta + \frac{1}{4L^2}\right)\right)\right]. \tag{47}$$

Additionally, as in the case (2), the growth rate is not influenced by k_z and the fastest growth rate is obtained when $k_x = 0$.

IV. NUMERICAL ANALYSIS

This section analyzes the zonal flow growth rate Γ [Eq. (42)] numerically. As the dependences on the various parameters are complicated and cannot be established analytically, we, thus, rely on numerical work to analyze the dependences of the growth rate on the different parameters zonal wave-vector q_x, β, and scale length L. The laboratory plasma is considered in our model,[3] with the magnetic field of B = 3G, number density $n_{0e} = 1 \times 10^{12}\,\mathrm{cm}^{-3}$, and electron temperature $T_e = 3 \times 10^2$ K.

Figure 1 shows that when q_x is increased, the zonal flow growth rate increases along with k_y. Plots are also made for other values of q_x that shows that it enhances the growth rate.

Figure 2 shows that growth rate increases with increasing values of $\beta = 1 + \frac{n_{po}}{Zn_{io}}(1 + \frac{T_e}{T_p})$, which indicates that positrons enhance growth by keeping $q_x = 0.6$ and keeping the other parameters the same as in Fig. 1.

It is found that $\beta = 1$ for E–I plasma, and the dependence of growth rate and k_y is shown in Figs. 2 and 3, which may be taken as a baseline graph. Furthermore, by increasing β to the values equal to 1.2, 1.5, 2, and 2.5, it is obvious from the graph (Fig. 2) that due to the increasing contribution of the positrons, the growth rate increases. Figures 3(a)–(c) illustrate the dependence of the growth rate on the scale length L for different values of β when the other parameters are kept constant. It is found that the growth rate increases as L increases.

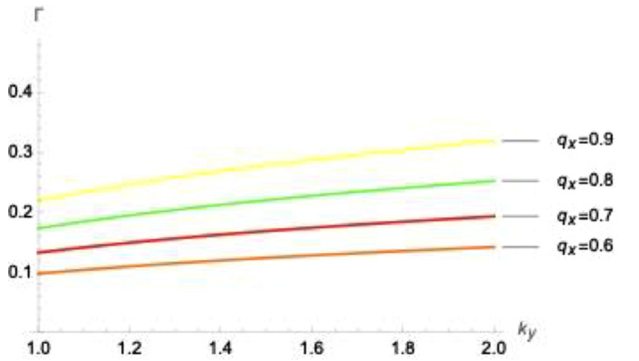

FIG. 1. Dependence of the zonal flow growth rate Γ vs k_y is shown for the following parameters: L = 1.5; $k_z = 0.1$; and $\beta = 1.2$.

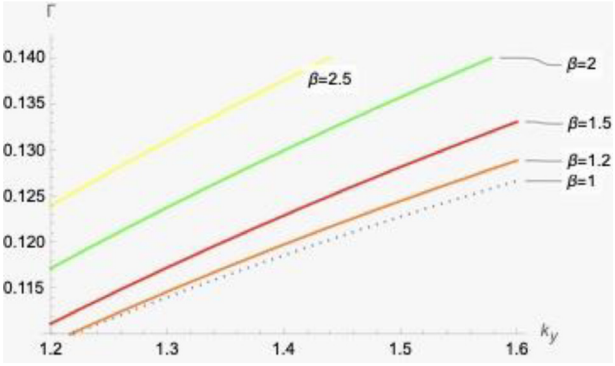

FIG. 2. Dependence of the zonal flow growth rate Γ vs k_y is shown for the following parameters: $q_x = 0.6$; L = 1.5; and $k_z = 0.1$.

In Fig. 3(a), the graph showing the absence of positrons and plasma appears as E-I at $\beta = 1$.

As shown in Figs. 3(b) and 3(c), the graph illustrates that when $\beta = 2$ and 3, the growth rate increases with k_y as the positron concentration increases. A comparison of Fig. 3(a) with Figs. 3(b) and 3(c) indicates that, as β increases, the crossing at $\beta = 1$ disappears with an increase in β, indicating the presence of positrons in plasma and enhancement of growth rate as well.

In Fig. 4, the zonal flow growth rate Γ are plotted against k_z. The plots are made for different values of the zonal flow wave number q_x, indicating that the growth rate increases as q_x increases.

According to Fig. 5, when values of β are changed, the growth rate Γ increases, while the growth rate Γ gets compressed on increasing the values of wave vector k_z.

Figures 6(a)–(c) explain the dependence of the growth rate on the scale length L at different values of β. It is found that by fixing other parameters, the growth rate increasing as L increases while at higher values of k_z, the growth rate Γ gets compressed.

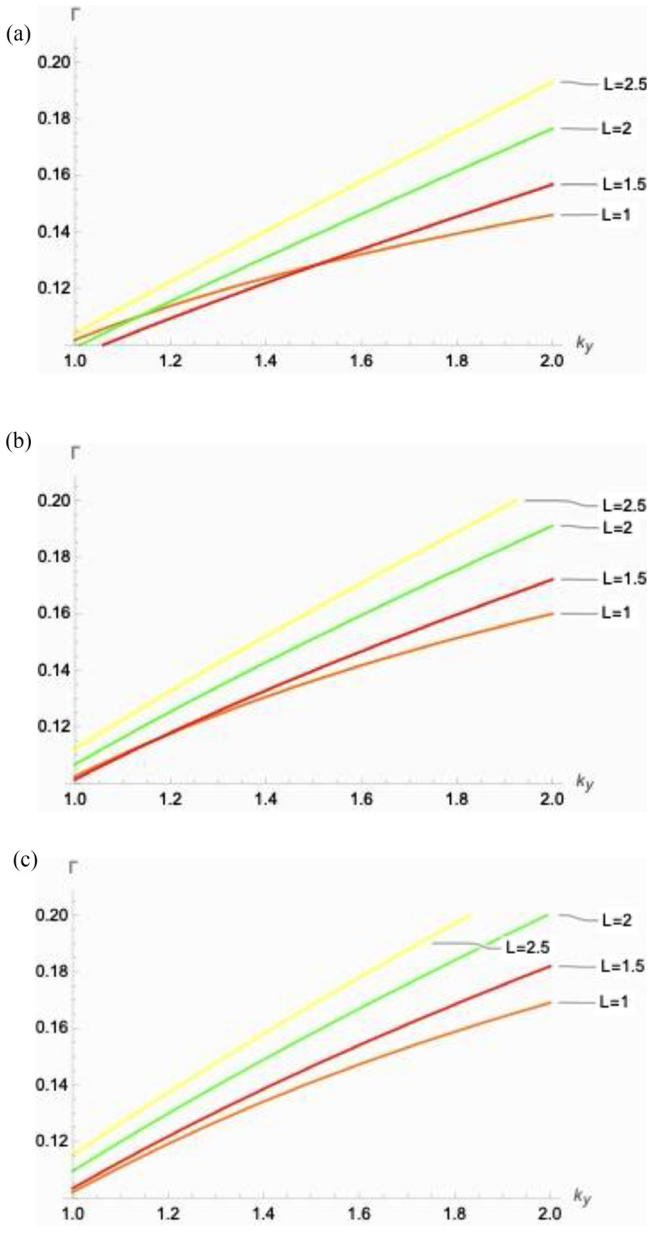

FIG. 3. (a) Dependence of the zonal flow growth rate Γ vs k_y is shown for the following parameters: $q_x = 0.6$; $k_z = 0.1$; and $\beta = 1$.(b) Dependence of the zonal flow growth rate Γ vs k_y is shown for the following parameters: $q_x = 0.6$; $k_z = 0.1$; and $\beta = 2$. (c) Dependence of the zonal flow growth rate Γ vs k_y is shown for the following parameters: $q_x = 0.6$; $k_z = 0.1$; and $\beta = 3$.

V. CONCLUSION AND DISCUSSION

In the present paper, the zonal flow generation driven by coupled low-frequency drift-ion-acoustic waves in laboratory EPI plasmas is investigated. Here, attention is given to the small-scale waves ($k_\perp \rho_s \gtrsim 1$); the carried out investigation provides an essential nonlinear mechanism for the spectral energy transfer from small-scale drift-ion-acoustic waves to large-scale enhanced zonal flows. The modified

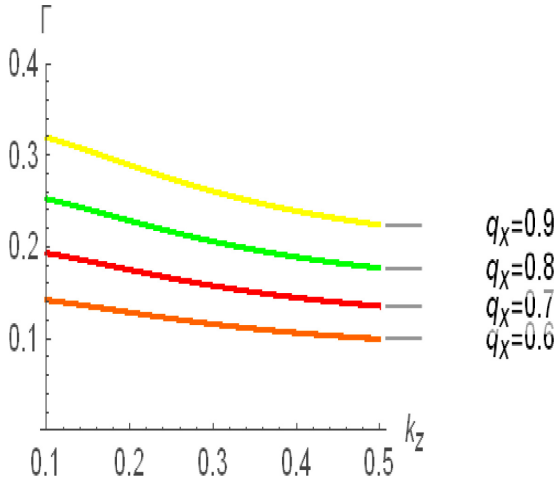

FIG. 4. Dependence of the zonal flow growth rate Γ vs k_z is shown for the following parameters: $L = 1.5$; $k_y = 2$; and $\beta = 1.1$.

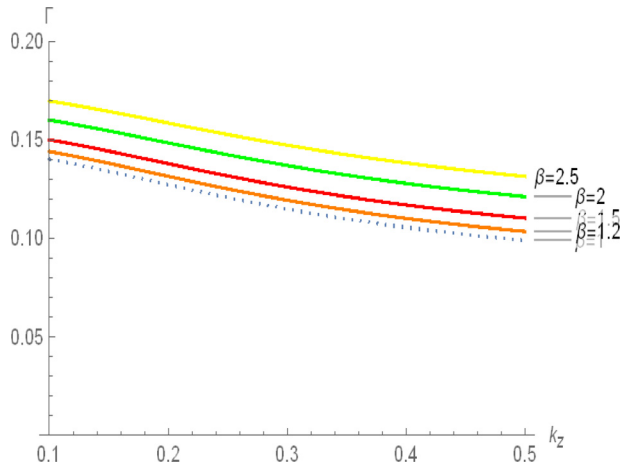

FIG. 5. Dependence of the zonal flow growth rate Γ vs k_z is shown for the following parameters: $q_x = 0.6$; $L = 1.5$; and $k_y = 2$.

parametric approach is developed for the monochromatic primary modes. Accordingly, the interaction of a pump drift-ion-acoustic waves, two satellites of the pump waves (sideband waves), and a sheared zonal flow is studied. The driving mechanism of this instability is the Reynold stress $r_\perp$ and the mean electromotive force $r_{\parallel}$. The obtained results are applied to laboratory plasma experiments[3,18–22] that were considered for the case when $k_\perp \rho_s \gtrsim 1$.

Section II describes the methodology and the mathematical formulation of dealing with the basic system of nonlinear equations [see Eqs. (5) and (6)] containing only vector nonlinearities for short-scale DIAWs. The linear regime of coupled drift-ion-acoustic waves is discussed, along with the limiting cases [see Eqs. (10)–(13)]. Section III discusses the generation of sheared zonal flows by coupled drift-ion-acoustic waves in electron–positron–ion plasmas. It is shown that the generation is due to the parametric excitation due to three-wave interaction, in which the coupling between the pump drift-ion-acoustic

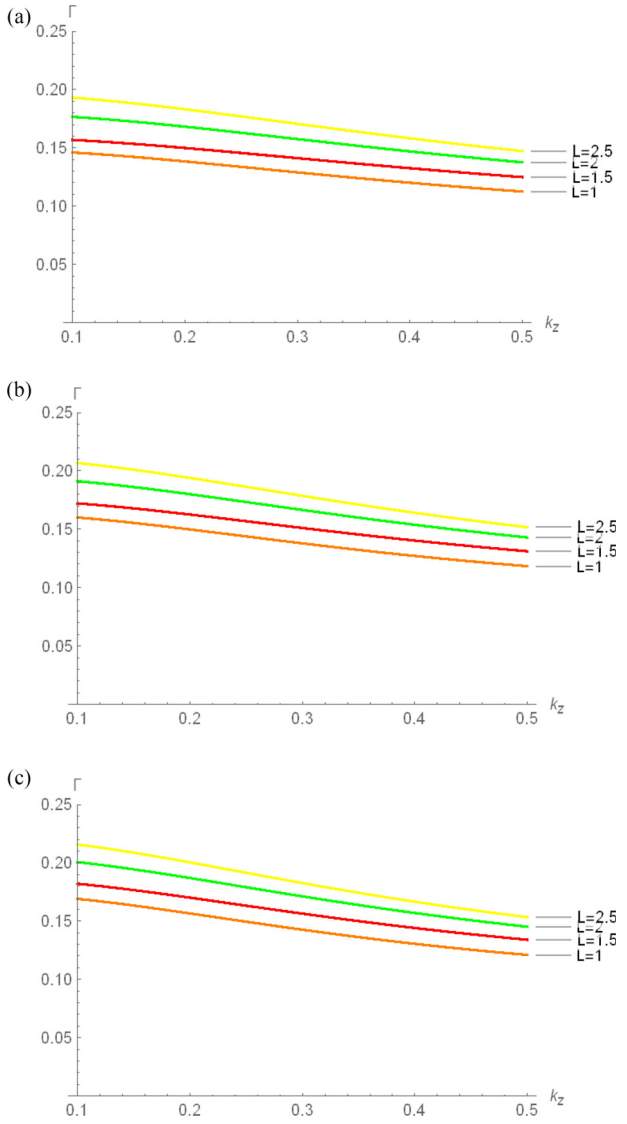

FIG. 6. (a) Dependence of the zonal flow growth rate Γ vs k_z is shown for the following parameters: $q_x = 0.6$; $k_y = 2$; and $\beta = 1$. (b) Dependence of the zonal flow growth rate Γ vs k_z is shown for the following parameters: $q_x = 0.6$; $k_y = 2$; and $\beta = 2$. (c) Dependence of the zonal flow growth rate Γ vs k_z is shown for the following parameters: $q_x = 0.6$; $k_y = 2$; and $\beta = 3$.

waves and sideband modes gives rise to large-scale modes, i.e., the zonal flows [see Eq. (18)]. The driving mechanism of the instability is due to the Reynolds stresses $r_\perp$ and the mean electromotive force $r_\parallel$ [see Eq. (19)] of the zonal flow.

The corresponding expressions for the growth rate are found for small-scale $(k_\perp \rho_s \gtrsim 1)$ pump structures [see Eqs. (41) and (42)]. Here, the vector nonlinearity plays the role under certain excitation conditions showing that the wave vector of fast mode is transverse to that of the drift-ion-acoustic pumping wave [see Eqs. (43) and (44)]. For the limiting cases, explicit relations have been obtained for the fastest growth rate [see Eqs. (45)–(47)], which shows that in comparison to usual electron ion plasma, the presence of positrons in the plasma gives modification in zonal flow growth rate as well as in instability conditions. Numerically, it is shown that for the laboratory plasma parameters for magnetized EPI plasmas, the growth rate is enhanced. The growth rate also increases with the increase in q_x and L.

The numerical estimation of growth rate is carried out from the analytical expressions Eqs. (43)–(47)

$$\Gamma \sim \omega_{ci} \left(\frac{q_x}{k_y}\right)^2 (k_y \rho_s)^3 \left|\frac{e\tilde{\varphi}_+}{T_e}\right|. \tag{48}$$

For the experimental data[3] $\omega_{ci} \sim 10^8 s^{-1}$; $k_y \rho_s \sim 5$; $\frac{e\tilde{\varphi}_+}{T_e} \sim 10^{-1}$; $\frac{q_x}{k_y} \sim 10^{-1}$, we get $\Gamma \sim 10^7 s^{-1}$. It is shown that such kinds of flows need excitation conditions and they are not spontaneously generated.

The novelty in the present investigation appears through the analytical and numerical results. In Ref. 7, the authors considered an electron–ion plasma and the effect of the polarization drift was neglected in comparison with the $\mathbf{E} \times \mathbf{B}$ drift. However, in this work, an EPI plasma along with polarization drift for zonal flow is investigated. The EPI plasmas, which are found abundantly in many naturally occurring and laboratory plasmas, have already been discussed in Sec. I. In the present work, the effect of positron density appears through the β term, which increases by increasing $\frac{T_e}{T_p}$ by fixing densities or by fixing $\frac{T_e}{T_p}$ and increasing $\frac{n_{po}}{Zn_{io}}$. It is found that by taking $(\beta + \frac{1}{4L^2}) = 1$, the growth rate as well as the instability conditions of Ref. 7 are retrieved. Thus, the mathematical results and graphical analysis in this paper highlight the importance of effects that have not been taken into account in earlier works.

This study shows that the parametric instability presented here is a sufficient nonlinear mechanism to drive large-scale zonal flows in EPI laboratory plasmas.[23,24] The results obtained in the present study may be applied to the large-scale inhomogeneities in density of the universe[25] and also to the astrophysical EPI jets,[26] where ions concentrations are taken as small fractions of the electron–positron plasma number densities.

AUTHOR DECLARATIONS

Conflict of Interest

The authors have no conflicts to disclose.

Author Contributions

Imran Javaid: Conceptualization (equal); Methodology (equal); Resources (equal); Writing – original draft (equal). **Laila Zafar Kahlon:** Conceptualization (equal); Methodology (equal); Software (equal); Supervision (equal); Writing – original draft (equal). **Hassan Amir Shah:** Conceptualization (equal); Methodology (equal); Writing – review & editing (equal). **Tamaz Kaladze:** Supervision (equal); Writing – review & editing (equal).

DATA AVAILABILITY

The data that support the findings of this study are available within the article.

REFERENCES

[1]P. K. Shukla, A. A. Mamun, and L. Stenflo, Phys. Scr. **68**, 295 (2003).
[2]A. M. Mirza and M. Azeem, Phys. Plasmas **11**, 4341 (2004).

[3]A. Mushtaq, Phys. Plasmas **15**, 082313 (2008).
[4]A. Mushtaq, R. Saeed, and Q. Haque, Phys. Plasmas **18**, 042305 (2011).
[5]L. Wang, P. H. Diamond, and T. S. Hahm, Plasma Phys. Controlled Fusion **54**, 095015 (2012).
[6]M. Adnan, S. Mahmood, and A. Qamar, Phys. Plasmas **21**, 092119 (2014).
[7]T. D. Kaladze, L. Z. Kahlon, and L. V. Tsamalashvili, Phys. Plasmas **24**, 072302 (2017).
[8]L. Z. Kahlon, I. Javaid, and T. D. Kaladze, Braz. J. Phys. **50**, 291 (2020).
[9]P. H. Diamond, S.-I. Itoh, K. Itoh, and T. S. Hahm, Plasma Phys. Controlled Fusion **47**, R35 (2005).
[10]A. Hasegawa and K. Mima, Phys. Rev. Lett. **39**, 205 (1977).
[11]A. Hasegawa and K. Mima, Phys. Fluids **21**, 87 (1978).
[12]V. I. Petviashvili, Pis'ma ZhETF **32**, 632 (1980); V. I. Petviashvili, JETP Lett. **32**, 619 (1980), available at http://jetpletters.ru/ps/1434/article_21816.pdf
[13]A. B. Mikhailovskii, "Vortices in plasma and hydrodynamics," in *Nonlinear Phenomena in Plasma Physics and Hydrodynamics*, edited by R. Z. Sagdeev (Mir Publishers, Moscow, 1986).
[14]M. V. Nezlin, Chaos **4**, 187 (1994).
[15]M. V. Nezlin and G. P. Chernikov, Plasma Phys. Rep. **21**, 922 (1995), available at https://ui.adsabs.harvard.edu/abs/1995PlPhR..21..922N
[16]L. Z. Kahlon and I. Javaid, Chin. Phys. Lett. **34**(12), 123201 (2017).
[17]T. D. Kaladze, M. Shad, and L. V. Tsamalashvili, Phys. Plasmas **17**, 022304 (2010).
[18]T. D. Kaladze, D. J. Wu, O. A. Pokhotelov, R. Z. Sagdeev, L. Stenflo, and P. K. Shukla, Phys. Plasmas **12**, 122311 (2005).
[19]A. Fujisawa, Phys. Rev. Lett. **93**, 165002 (2004).
[20]A. Mirza, A. Hasan, M. Azeem, and H. Saleem, Phys. Plasmas **10**, 4675 (2003).
[21]S. I. Popel, S. V. Vladimirov, and P. K. Shukla, Phys. Plasmas **2**, 716 (1995).
[22]V. V. Zheleznyakov and S. A. Koryagin, Astron. Lett. **31**, 713–728 (2005).
[23]R. G. Greaves and C. M. Surko, Phys. Rev. Lett. **75**, 3846–3849 (1995).
[24]M. D. Tinkle, R. G. Greaves, C. M. Surko, R. L. Spencer, and G. W. Mason, Phys. Rev. Lett. **72**, 352 (1994).
[25]M. J. Rees, in *The Very Early Universe*, edited by G. M. Gibbons, S. W. Hawking, and S. Siklas (Cambridge University Press, Cambridge, England, 1983).
[26]M. Honda and Y. S. Honda, Astrophys. J. Lett. **569**, L39 (2002).